Science on Form: Proceedings of the First International Symposium for Science on Form,
General Editor: S. Ishizaka, Editors: Y. Kato, R. Takaki, and J. Toriwaki, 219–228.

A Quantitative Analysis Method for Orientation of Fibrous Pattern

Masanori Idesawa and Takashi Soma

RIKEN, The Institute of Physical and Chemical Research, Wako-shi, Saitama 351-01, Japan

Keywords: index of orientation, fibrous pattern, trabecular pattern, direction of ridge, direction component of pattern boundaries

Orientations of fibrous pattern observed in a material are closely related to its mechanical properties. Several kinds of methods of analysis for the orientation of fibrous patterns are investigated. They give not only the measure of the direction of orientation but also that of the degree of ordering or alignment of the fibrous pattern. These measure should reflect the global or the average property in the area of interest. Two different types of methods are proposed. One is developed as an application of the ridge detection method for the fringe pattern analysis, in which the orientation is estimated as an average of the partial orientation of the ridge line in the area of interest. The other finds some model pattern which has the same direction component of pattern boundaries as that of the pattern under study and the orientation is estimated from the parameter specifying this model pattern. An architecture for the special purpose processing unit for these operations is also proposed.

1. Introduction

Orientation of fibrous micro patterns which are observed in materials such as boundaries of bond grains, grains of wood, fibers of cloths or papers, muscle fibers or trabecular pattern in bones and so on are closely related to the mechanical properties of the materials. These fibrous patterns are observed in an ordinary photograph, an X-ray photograph or a photograph taken under a microscope and so on. They have been used to investigate the characteristics of materials from a qualitative point of view so far.

Recently quantitative analysis of these patterns are required especially in the biomedical field. It seems doubtless that the trabecular pattern observed in a bone can be compared to the truss structure in a building and the bone of animals were constructed its optimum structure according to the load (Oda, J., (1981), Singh, M. et al., (1970)). Furthermore, some diseases are appeared as changes in density or orientation of fibrous pattern in a bone. It seems that these changes of fibrous patterns may be applied to investigate disease of a bone. However, quantitative analysis method has not been established so far.

In this paper, the authors aim to develop a simple method to analyze the orientation of fibrous patterns quantitatively, and to give an index of pattern orientation.

2. Relations between direction or density of fibrous pattern and characteristics of materials

Figure 1 shows a fibrous pattern observed in a head of human femur and its conceptual diagram of the load and the orientation of trabecular patterns. This picture was taken as a photograph of micro-radiogram by slicing a head of femur into a 50 μm thickness wafer. From these figures it can easily

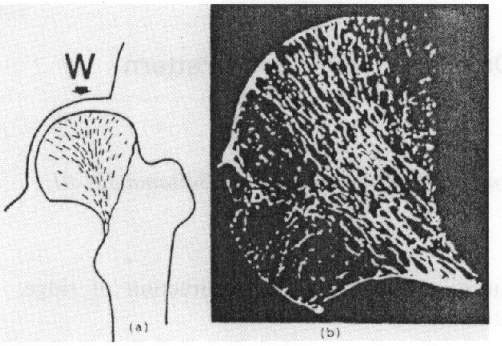

(a) Conceptual diagram of a femur and load
(b) Trabecular pattern observed in a head of femur

Fig.1 An example of trabecular pattern

be recognized that there are some relations between trabecular pattern orientation and its mechanical characteristics. However, an orientation of fibrous pattern is a very ambiguous concept, and has been discussed only in qualitative sense so far. In order to discuss orientations of fibrous pattern in quantitative sense, it is required to develop a quantitative analysis method of pattern orientation. It seems that the orientation of the pattern corresponds to the direction of the load or stress and the density of the pattern corresponds to the strength of the load or stress in the case of bone. Accordingly, if the effective analysis methods of the pattern orientation were established, a clue to quantitative analysis of mechanical characteristics related to pattern orientations or relations between disease and pattern change can be found.

3. Quantitative methods for analyzing orientation of fibrous pattern

It can be reminded that the method of estimating the pattern orientation from the direction of ridge lines or skeleton lines is possible. On the other hand, it must also be recalled that it is important to extract the macroscopical orientation in the area of interest and the microscopical orientation such as the direction of ridge line can not be a key parameter in the present subject.

It seems a probable method that estimate an orientation index from spatial frequencies in different directions calculated by filtering techniques, but is expected that this method requires a lot of computing time.

Therefore, a method to estimate an orientation by relating to the direction of the peak detection in the process of ridge detection for fringe pattern and a method to estimate the orientation in the area of interest from the direction components of binary pattern boundaries are proposed and investigated in this paper.

3.1 Method for detecting ridge line direction

Figure 2 shows a ridge point detection method which was developed to analyze the fringe patterns such as a moire pattern. The peak conditions shown in Fig.2 are examined to the direction X, Y, XY and YX in the 5 x 5 image points surrounding the interested point. The interested point is treated as a point on a ridge line when peak conditions are satisfied in more than one directions. The direction of the ridge line can be considered a direction which is perpendicular to that of the peak detection. The relations between the ridge line and the direction of the peak detection are summarized in Fig.3. For instance, if the peak condition is satisfied in the direction X and XY at the point of interest, the point is assumed as a point on a ridge line and the direction of the ridge line can be estimated as Y-YX direction which is perpendicular to the intermediate direction of X and XY. An average direction can be calculated by applying this ridge detection scheme to each

$P_{-2\,2}$	$P_{-1\,2}$	$P_{0\,2}$	$P_{1\,2}$	$P_{2\,2}$
$P_{-2\,1}$	$P_{-1\,1}$	$P_{0\,1}$	$P_{1\,1}$	$P_{2\,1}$
$P_{-2\,0}$	$P_{-1\,0}$	$P_{0\,0}$	$P_{1\,0}$	$P_{2\,0}$
P_{-2-1}	P_{-1-1}	P_{0-1}	P_{1-1}	P_{2-1}
P_{-2-2}	P_{-1-2}	P_{0-2}	P_{1-2}	P_{2-2}

(a) 5 x 5 mask for ridge detection

$$X\ \begin{cases} P_{00}+P_{0-1}+P_{01} > P_{-21}+P_{-20}+P_{-2-1} \\ \text{and} \\ P_{00}+P_{0-1}+P_{01} > P_{21}+P_{20}+P_{2-1} \end{cases}$$

$$Y\ \begin{cases} P_{00}+P_{-10}+P_{10} > P_{-1-2}+P_{0-2}+P_{1-2} \\ \text{and} \\ P_{00}+P_{-10}+P_{10} > P_{-12}+P_{02}+P_{12} \end{cases}$$

$$XY\ \begin{cases} P_{00}+P_{-1-1}+P_{11} > P_{-22}+P_{-21}+P_{-12} \\ \text{and} \\ P_{00}+P_{-1-1}+P_{11} > P_{2-2}+P_{2-1}+P_{1-2} \end{cases}$$

$$YX\ \begin{cases} P_{00}+P_{-11}+P_{1-1} > P_{22}+P_{21}+P_{12} \\ \text{and} \\ P_{00}+P_{-11}+P_{1-1} > P_{-2-2}+P_{-2-1}+P_{-1-2} \end{cases}$$

(b) Condition for peak detection

Fig.2 Ridge detection scheme

{ X, XY }	------->	Y-YX	-67.5 (θ_1 , N_1)
{ X, XY, Y }	------->	YX	-45.0 (θ_2 , N_2)
{ Y, XY }	------->	X-YX	-22.5 (θ_3 , N_3)
{ XY, Y, YX }	------->	X	0.0 (θ_4 , N_4)
{ Y, YX }	------->	X-XY	22.5 (θ_5 , N_5)
{ Y, YX, X }	------->	XY	45.0 (θ_6 , N_6)
{ X, YX }	------->	Y-XY	67.5 (θ_7 , N_7)
{ YX, X, XY }	------->	Y	90.0 (θ_8 , N_8)

Fig.3 Relation between ridge detection and peak detecting direction

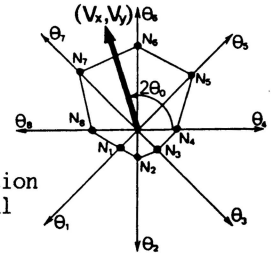

Fig.4 Frequency of ridge detection for each direction and conceptual diagram of averaging scheme

point and performing the averaging scheme shown in Fig.4. That is, supposing that Θ_i and N_i represent the angle and the ridge detection frequency for i-th direction respectively, and S represents the area of interested region. The average component (V_x, V_y), the average direction of orientation Θ_0 and its normalized length D (strength of orientation) can be calculated as follows,

$$V_x = \sum_{i=1}^{8} N_i \cos(\Theta_i), \quad V_y = \sum_{i=1}^{8} N_i \sin(\Theta_i),$$

$$D = \frac{\sqrt{V_x^2 + V_y^2}}{S}, \quad \Theta_0 = \frac{1}{2}\{\mathrm{sign}(V_y)(1 - \mathrm{sign}(V_x))\frac{\pi}{2} + \tan^{-1}(\frac{V_y}{V_x})\}. \qquad (1)$$

Where D : $(0<D<1)$ is a parameter related to the strength of orientation (orientation index) and D=0 means that the objective pattern has no orientation.

3.2 Method for estimating orientation from direction components of pattern boundaries

Figure 5 shows X and Y direction components of pattern boundary (L_x and L_y). From this figure we can easily understand that the direction component

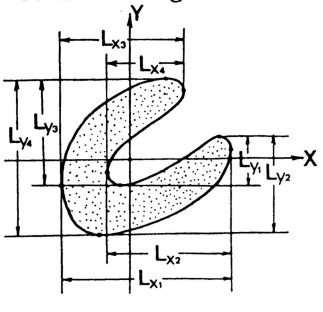

Fig.5 Direction components of pattern boundary as a shadow
$L_x=L_{x1}+L_{x2}+L_{x3}+L_{x4}$, $L_y=L_{y1}+L_{y2}+L_{y3}+L_{y4}$

of pattern boundaries is closely related to the orientation of the pattern. Therefore, it may be possible to estimate the orientation of a pattern from the direction components of the pattern boundaries. It seems difficult to detect the boundary line strictly, because it is required to trace the boundaries of the pattern and the high level recognitions are required. However, it seems easy to obtain the shadow component of the boundary direction for the binary pattern to particular direction. Therefore, some methods which estimate the pattern orientation from shadow components of the pattern boundaries to the axis X, Y, XY and YX (L_x, L_y, L_{xy} and L_{yx}) are investigated. One of them is an averaging method of directions and the others are method which replace shadow components to a typical pattern model. Direction and the strength of the pattern orientation are estimated by analyzing the parameters of the typical pattern. Figure 6 shows relations between each typical pattern model and components of direction of pattern boundaries.

3.2.1 Averaging method

In this method, adopted averaging scheme is based on entirely the same principle as shown in Fig.4. This corresponds to the case in which X-direction is 0°, Y-direction is 90° and YX-direction 45° and YX-direction is -45° in equations (1). Applying equation (1) to this case, strength of orientation D and the average direction Θ_0 are given by the following equations.

$$V_x = (L_x - L_y), \quad V_y = (L_{xy} - L_{yx}),$$

$$D = \sqrt{V_x^2 + V_y^2}, \quad \Theta_0 = \frac{1}{2}\{\mathrm{sign}(V_y)(1 - \mathrm{sign}(V_x))\frac{\pi}{2} + \tan^{-1}(\frac{V_y}{V_x})\}. \qquad (2)$$

This method is simple enough but pattern orientation can be estimated excellently.

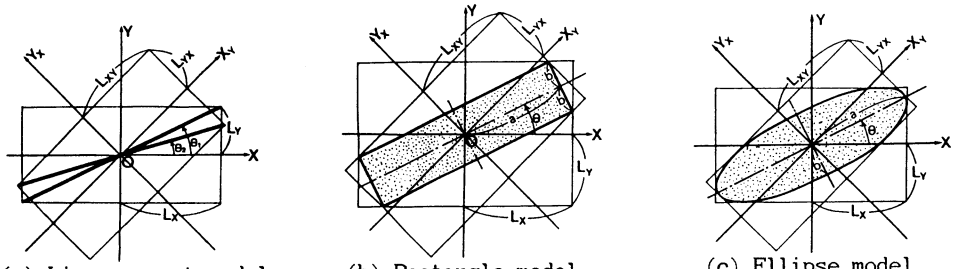

(a) Line segment model (b) Rectangle model (c) Ellipse model

Fig.6 Various models for pattern boundary matching

3.2.2 Line segment model

In this model, direction components of pattern boundaries are replaced by an equivalent line segment. If the original image are composed only from line segments, line segment model corresponding to L_x,L_y, and L_{xy},L_{yx} are to be coincident with each other (Fig.6a). However, usual patterns are composed not only from line segments, it is often occurred that the two line segment models does not coincide with each other. Because of this reasons, direction is estimated as a weighted average of these two directions. The strength of the orientations are given as follows,

$$V_x = (L_x - L_y), \quad V_y = (L_{xy} - L_{yx}), \quad D = \sqrt{V_x^2 + V_y^2}, \quad \Theta = \frac{V_x^2\Theta_1 + V_y^2\Theta_2}{V_x^2 + V_y^2}. \quad (3)$$

Where Θ_1 and Θ_2 are given according to the relations between L_x and L_y or L_{xy} and L_{yx} as follows:

(1) for $V_x<0$ and $V_y>0$, $\Theta_1 = \frac{\pi}{2} - \tan^{-1}(\frac{L_x}{L_y})$, $\Theta_2=\frac{\pi}{4} + \tan^{-1}(\frac{L_{yx}}{L_{xy}})$;

(2) for $V_x>0$ and $V_y>0$, $\Theta_1 = \tan^{-1}(\frac{L_y}{L_x})$, $\Theta_2 = \frac{\pi}{4} + \tan^{-1}(\frac{L_{yx}}{L_{xy}})$;

(3) for $V_x>0$ and $V_y<0$, $\Theta_1 = -\tan^{-1}(\frac{L_y}{L_x})$, $\Theta_2 = -\frac{\pi}{4} + \tan^{-1}(\frac{L_{yx}}{L_{xy}})$;

(4) for $V_x<0$ and $V_y<0$, $\Theta_1 = -\frac{\pi}{2} + \tan^{-1}(\frac{L_x}{L_y})$, $\Theta_2 = -\frac{\pi}{4} + \tan^{-1}(\frac{L_{xy}}{L_{yx}})$.

3.2.3 Rectangle model

In this method components of pattern boundaries are applied to a rectangle which has $2a$ length and $2b$ width and is inclined Θ as shown in Fig.6b. Parameters a, b and Θ can be estimated as below. Now replace b as $b=ka$, the following relations are given.

$$L_x = a(\cos\Theta + k\sin\Theta), \quad L_y = a(\sin\Theta + k\cos\Theta),$$

$$L_{xy} = a\{\cos(\Theta-\frac{\pi}{4}) + k\sin(\Theta-\frac{\pi}{4})\}, \quad L_{yx} = a\{\sin(\Theta-\frac{\pi}{4}) + k\cos(\Theta-\frac{\pi}{4})\}. \quad (4)$$

Solving these equations for a, Θ and k and represent the strength of orientation D equal to $(a-b)$, we have

$$D = \frac{\sqrt{(L_x-kL_y)+(L_y-kL_x)}}{1 + k}. \quad (5)$$

Using a function K as $K(a,b,c,d) = (\sqrt{2}L_x+aL_{xy}+bL_{yx})/(\sqrt{2}L_y+cL_{xy}+dL_{yx})$, k and Θ are given according to the relations between L_x and L_y or L_{xy} and L_{yx} as follows:

(1) for $L_x<L_y$ and $L_{xy}>L_{yx}$,

$k = \sqrt{K(-1,+1,+1,-1)\ K(-1,-1,+1,+1)}$, $\Theta = \frac{\pi}{2} - \tan^{-1}(\frac{L_x-kL_y}{L_y-kL_x})$;

(2) for $L_x>L_y$ and $L_{xy}>L_{yx}$,

$k = \sqrt{K(-1,-1,+1,+1)\ K(-1,+1,+1,-1)}$, $\Theta = \tan^{-1}(\frac{L_y-kL_x}{L_x-kL_y})$;

(3) for $L_x>L_y$ and $L_{xy}<L_{yx}$,

$k = \sqrt{K(-1,-1,+1,+1)\ K(+1,-1,-1,+1)}$, $\Theta = -\tan^{-1}(\frac{L_y-kL_x}{L_x-kL_y})$;

(4) for $L_x<L_y$ and $L_{xy}<L_{yx}$,

$$k = \sqrt{K(+1,-1,-1,+1)\ K(-1,-1,+1,+1)}\ ,\quad \Theta = -\frac{\pi}{2} + \tan^{-1}\left(\frac{L_x - kL_y}{L_y - kL_x}\right).$$

It seems that the rectangle model can give more suitable result than the line segment model.

3.2.4 Ellipse model

In this case, the components of boundary direction L_x, L_y, L_{xy} and L_{yx} applied to an ellipse which has the long principal axis a with angle Θ to X-direction and the short principal axis b as shown in Fig.6c. It can easily be shown that

$$a^2 = \frac{L_x^2 + L_y^2 + \sqrt{(L_x^2 - L_y^2)^2 + (L_{xy}^2 - L_{yx}^2)^2}}{2},$$

$$b^2 = \frac{L_x^2 + L_y^2 - \sqrt{(L_x^2 - L_y^2)^2 + (L_{xy}^2 - L_{yx}^2)^2}}{2},$$

$$\Theta = \frac{1}{2}\left\{\mathrm{sign}(L_{xy} - L_{yx})(1 - \mathrm{sign}(L_x - L_y))\frac{\pi}{2} + \tan^{-1}\left(\frac{L_{xy}^2 - L_{yx}^2}{L_x^2 - L_y^2}\right)\right\}. \qquad (6)$$

Furthermore, the strength of orientation can be given as either $D=(a-b)$ or $D=\sqrt{a^2-b^2}$. But different forms are also possible.

3.2.5 A practical method to estimate direction component of pattern boundaries

Figure 7 shows an example of a practical scheme to estimate direction components of pattern boundaries schematically. Selecting a mask corresponding to each direction as shown in Fig.7, and moving these mask in each direction step by step in the area of interest, then counting the turning frequency (black to white or white to black) in the direction along to the mask. For X and Y direction, turning frequencies are assigned to each component of boundary direction. For XY and YX direction, some compensations are required to make them equivalent value to that of X or Y direction. In the case of octagon mask (Fig.7), the scanning in X, Y, XY and YX direction is performed; the sum of turning frequency for each direction in the area of interest N_x, N_y, N_{xy} and N_{yx} are obtained; the compensated and normalized direction components of pattern boundaries are given as follows,

$$N_n = N^2 - 8(n-m)^2,\quad N_m = M^2 - 2(2m-n)^2,$$

$$L_x = \frac{N_x}{N_n},\quad L_y = \frac{N_y}{N_n},\quad L_{xy} = \frac{N_{xy}}{\sqrt{2}N_m},\quad L_{yx} = \frac{N_{yx}}{\sqrt{2}N_m} \qquad (7)$$

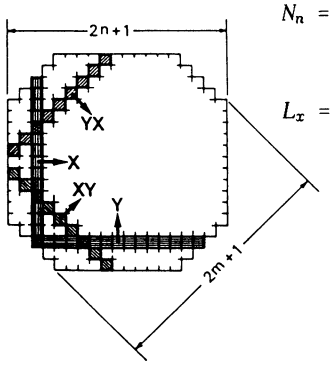

Fig.7 An example of practical method to estimate direction component of pattern boundaries as a shadow

4. A special purpose processing unit

Before showing the results of numerical experiment, let us consider the architecture of a special purpose processing unit for the above proposed method of analysis. Figure 8 shows a block diagram of the unit performing the operation described in 3.2.5. In the frame buffer of 512 by 512, for example, of binary picture there provided special windows for X, Y, XY and YX scanning direction, through which the image data are staticized simultaneously into the temporary memory (staticizing memory). The content of the memory is read columnwise (corresponding to the data for each scan line) into the shift register type memory and exclusive-or is taken between the successive data to count the number of changes in bit pattern. The number of ones is counted by the following side-way-adder (SWA) and accumulated in the accumulator (ACC). After the whole data in the memory are processed the data in the accumulator are sent to the output memory. This operation is performed in parallel for each memory of respective scan direction and ends at the same time when the data for next interested area come under the sampling window, so the complete

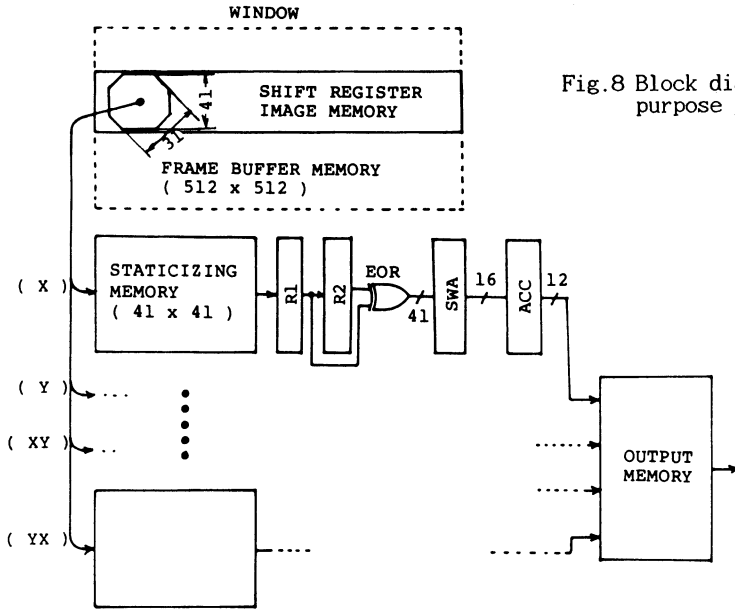

Fig.8 Block diagram of special purpose processing unit

cycle ends in one frame cycle. Assuming the frame rate of 30 frames per sec the bit rate will be the order of 100 nsec which value is not unrealistic to the present day CMOS technology. We think that this scheme is worth while considering for realization on one VLSI chip though a bit complicated.

5. Experiments

We tried to apply the proposed methods to analyze the orientation of trabecular pattern in a bone shown in Fig.1. A trabecular pattern picture was digitized into 512 by 512 image elements in 256 level gray scale. Figure 9a shows an example of ridge detection performed by using the method shown in Fig.2. Display of pattern orientation estimated from the ridge direction is shown in Fig.9b.

Figure 10 shows one of the test pattern to evaluate each orientation detection scheme and Figure 11 shows the display of the detected orientations by each scheme of the second type. In these figure the direction and the

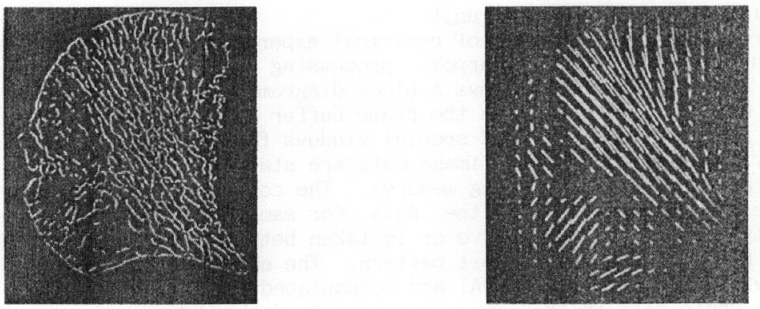

(a) Ridge detection

(b) Pattern orientation estimated from ridge direction

Fig.9 An example of ridge direction method

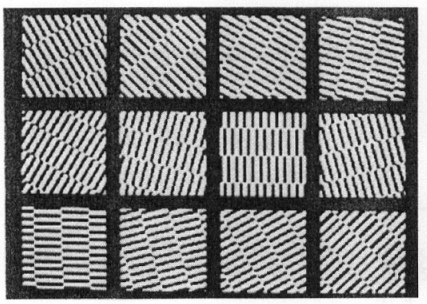

Fig.10 An example of test pattern for evaluation of orientation detection

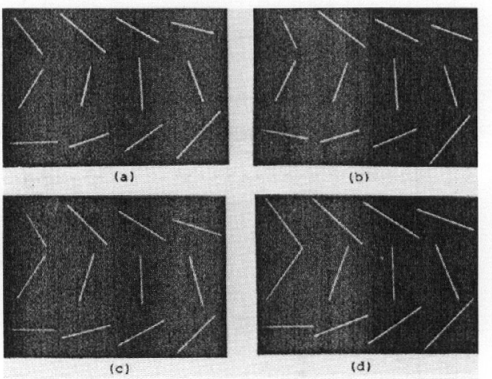

Fig.11 An example of orientation detection by each scheme for the test pattern shown in Fig.10 {(a) averaging, (b) line segment, (c) rectangle and (d) ellipse}

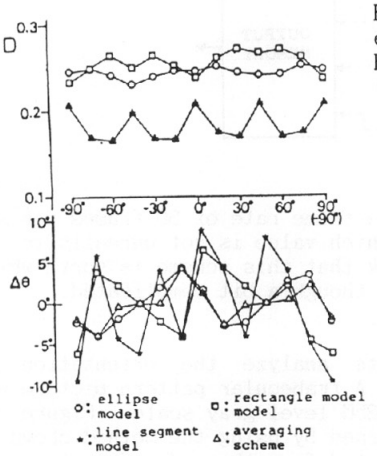

Fig.12 An example of orientation index and angle deviation estimated by each model for test pattern shown in Fig.10

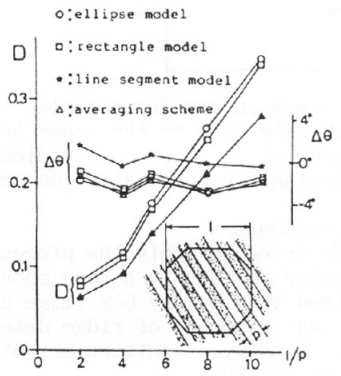

Fig.13 An example of strength of orientation and angle deviation against length-width ratio L/P of element pattern

length of the line segment represent the orientation and its strength respectively. The strength of orientation takes the value between 0 and 1, and takes 0 when the pattern has no orientation and 1 when at maximum strength. In this experiment, N and M are selected 41 and 31, respectively. Each result shows a fairly good agreement with the orientation of the test pattern shown in Fig.10.

Since in the method shown in Fig.2, the orientations are estimated from the partial direction of ridges and the partial orientations are applied to 8 directions, thus the orientations deviates considerably when the area of interest is selected small or patterns in the area is very rare.

On the other hand, the estimated orientations are fairly stable in the case of averaging or ellipse model, in spite of the estimation process is simple enough. Furthermore, the ellipse model method has the possibilities to select various indexes of orientation by using parameters of an ellipse a, b and θ in different forms. Thus, we can change the physical meaning of the strength of orientation and so on. Figure 12 shows an example of the orientation index and the angle deviation estimated by applying each model to the test pattern shown in Fig. 10. In this case, the strength of orientation deviates at 45° and at 135°. This reason can be expected because of the relation between digitizing grids and the test pattern orientation but the details are remained as a future subject.

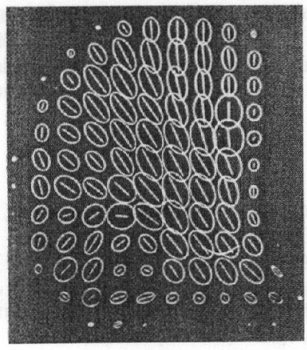

Fig.14 An example of estimated ellipse model and their orientation for trabecular pattern shown in Fig.1b

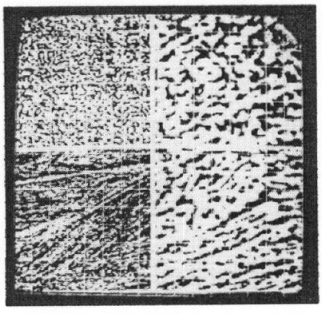

(a) Grain boundary pattern observed in Fe-C two-component metal

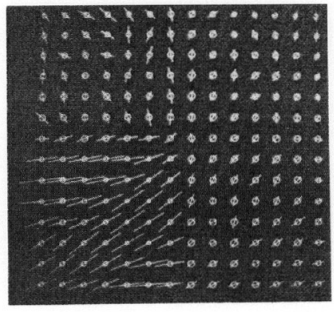

(b) Pattern orientation by ellipse model

Fig.15 An example of results obtained by method of ellipse model

Figure 13 shows an example of the strength of the orientation and the angle deviation against the length-width (pitch) ratio (L/P) of the element pattern. Figure 14 and Fig.15b show an example of the ellipse models estimated from Fig.1b and Fig.15a, respectively, and the strength of the orientation $D=\sqrt{a-b}$ are superimposed. Quantitative relations between each method have been under investigation, and it is a subject for future study.

6. Conclusion

In this paper the authors proposed the methods for analyzing the pattern orientation which give not only the measure of the direction of orientation (the angle of orientation) but also that of the ordering (the index of orientation) for the fibrous patterns. This method enables us to make a quantitative analysis of the pattern orientation and it becomes possible to obtain the relation between pattern orientations and its material characteristics such as mechanical or electrical property, etc. which have so far been discussed only in qualitative sense. The proposed method have been applied to the quantitative study of the relation between the condition of illness and the changes in trabecular pattern of the upper end of the femur, and a fairly good results have been obtained. Also an architecture for the special purpose processing unit for these operations is proposed.

The authors gratefully acknowledge the helpful discussion with Dr. T. Yatagai of University of Tsukuba and the trabecular pattern of femur and the medical comments from Prof. Y. Miura and Mr. S. Okita of Tokyo Medical University. They also express their appreciation to Mr. T. Abe of the Technical Division and the members of the Information Science Laboratory of Riken for their cooperation.

REFERENCES

Idesawa,M. and Yatagai,T.(1980): 3-D shape input and processing by moire technique, Proc. 5-th ICPR, p1085.

Idesawa,M., Yatagai,T., Okita,S. and Miura,Y. (1981): An analysis method of ridge pattern of a bone, Proc. 23-th Meeting of JIPS, p737.

Oda,J., (1981):Life and machine from view point of strength, Jour. Study of Machinery, vol.33, no.6, p27 (in Japanese).

Singh,M., Nagrath,A.R. and Maini,P.S.(1970):Changes in trabecular pattern of the upper end of femur as an index of osteoporosis, JBJS, vol.52-A, no.3, p457.